

Ion-size effect on normal-state transport properties in $R_{0.8}\text{Pr}_{0.2}\text{Ba}_2\text{Cu}_3\text{O}_{7-y}$ systems ($R = \text{Yb, Er, Dy, Gd, Eu, and Nd}$)

J. C. Chen

Department of Physics, National Tsing Hua University, Hsinchu, Taiwan, Republic of China

Yunhui Xu

Institut für Angewandte Physik, Universität Giessen, Heinrich-Buff-Ring 16, 35392 Giessen, Germany

M. K. Wu

Materials Science Center and Department of Physics, National Tsing Hua University, Hsinchu, Taiwan, Republic of China

Weiyan Guan

Department of Physics, Tamkang University, Tamsui, Taiwan, Republic of China

(Received 8 September 1995)

We report detailed studies of the normal-state resistivity and the Hall-effect in bulk $R_{0.8}\text{Pr}_{0.2}\text{Ba}_2\text{Cu}_3\text{O}_{7-y}$ samples ($R = \text{Yb, Er, Dy, Gd, Eu, and Nd}$). We find a linear temperature dependence of the normal-state resistivity ρ_n and the Hall number n_H above T_c in these systems. At a constant temperature both ρ_n and n_H are linearly dependent on the ion-size of the rare earth, viz., the larger R^{3+} ionic radius, the larger ρ_n , but the lower n_H . The cotangent of the Hall angle follows a universal T^2 dependence, i.e., $\cot\theta_H = \alpha T^2 + C$. Both the slope α and the quantity C is insensitive to the R ion and remains almost constant. On the basis of our data we propose a T_c - n_H diagram which manifests an “underdoping” behavior of $R_{0.8}\text{Pr}_{0.2}\text{Ba}_2\text{Cu}_3\text{O}_{7-y}$ systems. We suggest that the strong hybridization between the $4f$ states of the Pr ion and the conduction-band states in CuO_2 planes, leading to hole localization and pair breaking, are the mechanism for the suppression of superconductivity in $R_{1-x}\text{Pr}_x\text{Ba}_2\text{Cu}_3\text{O}_{7-y}$ systems.

I. INTRODUCTION

$\text{PrBa}_2\text{Cu}_3\text{O}_7$ is an intriguing exception among the rare-earth substituted isomorphous $\text{YBa}_2\text{Cu}_3\text{O}_7$ compounds due to the absence of superconductivity as well as a metallic state.¹ Specific heat and magnetization measurements² on $\text{PrBa}_2\text{Cu}_3\text{O}_7$ showed an anomalous magnetic ordering at $T_N = 17$ K. Neutron diffraction³ experiment suggested that this ordering is a three-dimensional antiferromagnetic order in the Pr sublattice. One approach in understanding these striking properties of $\text{PrBa}_2\text{Cu}_3\text{O}_7$ is to study in detail the effect of Pr doping in $R\text{Ba}_2\text{Cu}_4\text{O}_7$ compounds.¹

The attractiveness of these systems is that the continuous composition range, $0 \leq x \leq 1$, of solid solution formed in the $R_{1-x}\text{Pr}_x\text{Ba}_2\text{Cu}_3\text{O}_{7-y}$ systems based on different R provides a unique possibility to study the superconducting and magnetic subsystem interference.¹

We have carried out systematic study of the effect by Pr doping in $R_{1-x}\text{Pr}_x\text{Ba}_2\text{Cu}_3\text{O}_{7-y}$ systems ($R = \text{Lu, Yb, Tm, Er, Y, Ho, Dy, Gd, Eu, Sm, and Nd}$).⁴⁻⁶ It is found that at a critical Pr concentration, x_{cr} , the superconductivity is completely quenched, beyond which the system becomes insulating and displays magnetic ordering of the Pr sublattice. We observed a rare-earth ion size effect on T_c , T_N , and x_{cr} in these systems.

In Pr concentration region of $x < x_{\text{cr}}$, the superconducting transition temperature T_c decreases linearly with increasing Pr concentration, and that at a given Pr concentration, T_c decreases linearly with increasing the radius of R ion.⁴

On the other hand, in Pr concentration region of $x > x_{\text{cr}}$,

the magnetic ordering temperature T_N of the Pr ions decreases linearly with increasing R concentration. At a given R concentration, T_N decreases linearly with decreasing the radius of R ion.⁵

We observed that the critical Pr concentration x_{cr} also decreases linearly with increasing the radius of R ion.⁴ The observed results were interpreted in terms of the hybridization between the local states of Pr ion and the valence band states of the CuO_2 planes.⁶

One of the most puzzling problems in the study of high- T_c superconductors has been the anomalous linear temperature dependence of their normal-state resistivity ρ_n and the Hall number n_H above T_c ,⁷ which is inconsistent with an isotropic single-band Fermi-liquid description. A theory in the framework of the two-dimensional Luttinger liquid was proposed by Anderson,⁸ who argues that the intrinsic electronic freedom in CuO_2 planes is decomposed into two types of quasiparticle excitations, spin- $\frac{1}{2}$ chargeless spinons and charged spinless holons. The relaxation times for carrier motion normal to the Fermi surface and parallel to it are differentiated. The predicted T^2 -dependence of the Hall angle has been observed in many high- T_c cuprate superconductors.⁹⁻¹⁴

Extensive studies of the Hall effect have been carried out on the following 123-systems: (1) $\text{YBa}_2\text{Cu}_3\text{O}_{7-\delta}$ with changing the oxygen content δ ;^{9,10} (2) $\text{Y}_{1-x}\text{Pr}_x\text{Ba}_2\text{Cu}_3\text{O}_{7-\delta}$ with changing the Pr content x ;¹¹ and (3) $\text{YBa}_2\text{Cu}_{3-x}\text{M}_x\text{O}_{7-\delta}$ with changing the transition metal content x .¹²⁻¹⁴

All of the Hall experiments above⁹⁻¹⁴ have focused on the change of the concentration x of the dopants (Zn, Co, Fe, Pr) or the oxygen reduction δ . In modification of our previous

observation that the R^{3+} ion size has a very strong effect on superconducting and magnetic properties in $R_{1-x}\text{Pr}_x\text{Ba}_2\text{Cu}_3\text{O}_{7-y}$,⁴⁻⁶ we carried out present Hall measurements in $R_{0.8}\text{Pr}_{0.2}\text{Ba}_2\text{Cu}_3\text{O}_{7-y}$ systems, in which instead of changing the concentration, we change the R^{3+} ion while leaving the concentration of Pr and oxygen unchanged.

In this paper we report detailed studies of the normal state resistivity and Hall effect of bulk $(R_{0.8}\text{Pr}_{0.2})\text{Ba}_2\text{Cu}_3\text{O}_{7-y}$ ($R = \text{Yb, Er, Dy, Gd, Eu, and Nd}$). We find a linear temperature dependence of the resistivity ρ_n and the Hall number n_H above T_c in these systems. The cotangent of the Hall angle follows a universal T^2 dependence, namely, $\cot \theta = \alpha T^2 + C$. Both the slope α and the quantity C remain almost constant and are insensitive to the change of R ion in $R_{0.8}\text{Pr}_{0.2}\text{Ba}_2\text{Cu}_3\text{O}_{7-y}$. We find a rare-earth ion size effect on resistivity ρ_n and the Hall number n_H . At a constant temperature the resistivity ρ_n and the Hall number n_H is linearly dependent on R^{3+} ionic radius, the larger R^{3+} ionic radius, the larger ρ_n , but the lower n_H . Based on our data we proposed a T_c - n_H diagram which manifests an underdopinglike behavior of $R_{0.8}\text{Pr}_{0.2}\text{Ba}_2\text{Cu}_3\text{O}_7$ ($R = \text{Yb, Er, Dy, Gd, Eu, and Nd}$) systems.

II. EXPERIMENTAL

The ceramic $R_{0.8}\text{Pr}_{0.2}\text{Ba}_2\text{Cu}_3\text{O}_{7-y}$ ($R = \text{Yb, Er, Dy, Gd, Eu, and Nd}$) samples were synthesized using a conventional solid state reaction method. Stoichiometric amounts of high purity $R_2\text{O}_3$ ($R = \text{Yb, Er, Dy, Gd, Eu, and Nd}$), Pr_6O_{11} , BaCO_3 and CuO powders were mixed, ground and calcined at 915°C for about 24 h in air in Al_2O_3 crucibles, followed by slow cooling in the furnace. The resultant powder was then reground again and pressed with about 3 tons/cm^2 into pellets which was then heated at $925\text{--}935^\circ\text{C}$ for 3 days in flowing oxygen, followed by annealing at 680°C for 10 h and then slow cooled to 420°C , where they remained for 20 h before a final slow cool to room temperature. All specimens were annealed in an atmosphere of flowing oxygen to ensure a sufficient oxygen content in the final product. This sinter procedure was repeated at least three times. All samples were prepared at the same time in the same furnace as much as to ensure the same sample qualities. The structures of the samples were investigated using a Rigaku Rotaflex rotating anode powder x-ray diffractometer ($\text{CuK}\alpha$ radiation) at scanning rate of 4° in 2θ per minute.

The dc magnetization for each sample was measured by a Quantum Design magnetometer. To measure the Hall effect and the longitudinal resistivity a five-probe arrangement was used on rectangular shaped samples. The rectangular samples were cut from sintered pellets with typical dimensions $2 \times 5 \times 0.5 \text{ mm}$.³ In order to perform precise Hall measurements, it was essential to minimize the misalignment of the Hall arms and also to achieve low-resistance Ohmic contacts. The contacts were made using gold wires and silver epoxy. After a heat treatment of 2 h at 450°C in flowing oxygen the contact resistance was typically less than 0.5Ω for contact surfaces smaller than 0.1 mm^2 . Samples were mounted on small sapphire substrates.

In order to measure V_{xx} and V_{xy} simultaneously three voltage contacts were attached on each sample and recorded with two sensitive digital nanovoltmeters (Keithley 182).

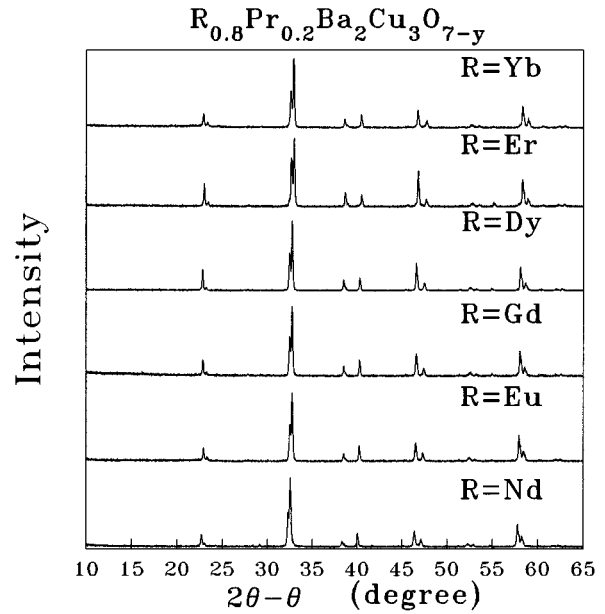


FIG. 1. X-ray powder diffraction patterns with $\text{CuK}\alpha$ radiation for $R_{0.8}\text{Pr}_{0.2}\text{Ba}_2\text{Cu}_3\text{O}_{7-y}$ ($R = \text{Yb, Er, Dy, Gd, Eu, Nd}$).

The experiments were performed in a commercial Oxford dewar with a superconducting magnet. The Hall voltage was obtained with a measuring current of 100 mA, which roughly corresponded to $J \approx 10\text{--}40 \text{ A cm}^{-2}$. To extract the Hall voltage a signal was measured at two reversal directions of the measuring current and two reversal directions of the magnetic field ($\pm 7 \text{ T}$). The temperature dependence of the longitudinal resistivity in zero field was measured in a separate run. The temperature was measured by a carbon glass thermometer (Lake Shore carbon resistor type 500) inside the sample chamber with an Oxford ITC4 temperature controller.

III. RESULTS AND DISCUSSION

The x-ray diffraction patterns at room temperature (Fig. 1) show that all samples have the layered orthorhombic perovskitelike structure and contain no extra peaks due to impurity phases within the experimental error. However, the orthorhombicity i.e., the e parameter, defined as $e = 2(b-a)/(b+a)$, decreases with increasing R^{3+} radius. The main peak split is not obvious for sample $\text{Nd}_{0.8}\text{Pr}_{0.2}\text{Ba}_2\text{Cu}_3\text{O}_{7-y}$ (Fig. 1). The lattice parameters a , b , c and the unit cell volume V of all samples are increasing monotonically with radius of R^{3+} ion.

The temperature dependence of the dc molar magnetization $M(T)$ of $R_{0.8}\text{Pr}_{0.2}\text{Ba}_2\text{Cu}_3\text{O}_{7-y}$ ($R = \text{Yb, Er, Dy, Gd, Eu, and Nd}$) systems over the temperature region $5\text{--}90 \text{ K}$ were measured both in zero field cooling (ZFC) and field cooling (FC). The results are shown in Fig. 2 (only for ZFC). The $M(T)$ curves demonstrate a superconducting transition. In ZFC measurements, in some samples there are a “knee” on the transition curves. It could be due to the granular character of the sintered samples. The transition of sintered pellets could be divided as a two-step process with firstly the transition of grains and followed by the transition of intergrain

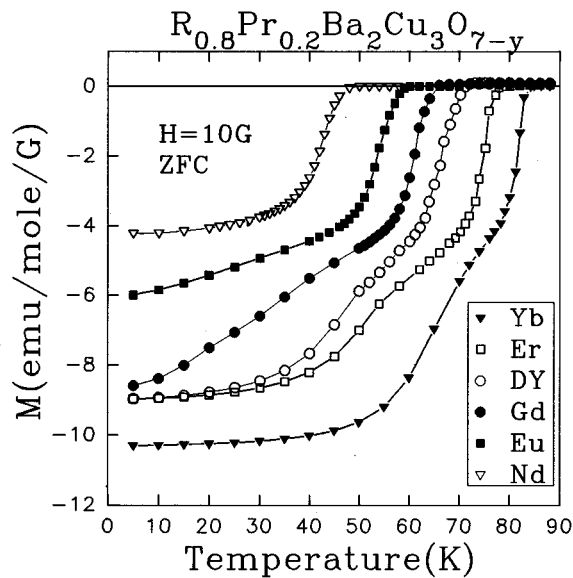


FIG. 2. Temperature dependence of dc molar magnetization for $R_{0.8}\text{Pr}_{0.2}\text{Ba}_2\text{Cu}_3\text{O}_{7-y}$ ($R=\text{Yb, Er, Dy, Gd, Eu, Nd}$).

barriers or junctions. The “knee” disappeared when we ground the bulk and performed the powder dc magnetic measurements.

Normal state resistivity ρ_n was measured in the temperature range between T_c and 290 K (Fig. 3). The results indicate that all samples are “metallic” with a linear temperature dependence of ρ_n . The resistivity at 280 K changes from 700 $\mu\Omega$ cm for $\text{Yb}_{0.8}\text{Pr}_{0.2}\text{Ba}_2\text{Cu}_3\text{O}_{7-y}$ to 1700 $\mu\Omega$ cm for $\text{Nd}_{0.8}\text{Pr}_{0.2}\text{Ba}_2\text{Cu}_3\text{O}_{7-y}$. For all $R_{0.8}\text{Pr}_{0.2}\text{Ba}_2\text{Cu}_3\text{O}_{7-y}$ samples the slopes of $\rho_n(T)$ curves have a same value of ≈ 2 $\mu\Omega$ cm/K (Fig. 3).

Figure 4 demonstrated that T_c (onset) decreases approximately linearly with increasing radius of R^{3+} ions. This is consistent with our previous reports.⁴ T_c values obtained from both resistivity and magnetization measurements are in good agreement with each other. It is the most striking aspect of these data that at a constant temperature (150 and 200 K

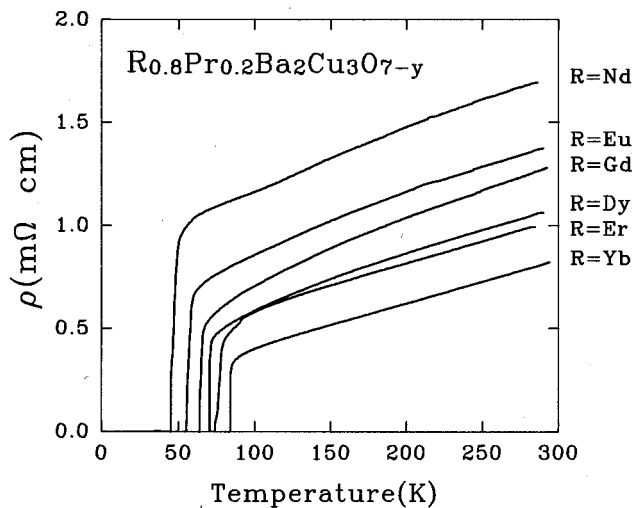


FIG. 3. Temperature dependence of resistivity ρ for $R_{0.8}\text{Pr}_{0.2}\text{Ba}_2\text{Cu}_3\text{O}_{7-y}$ ($R=\text{Yb, Er, Dy, Gd, Eu, Nd}$).

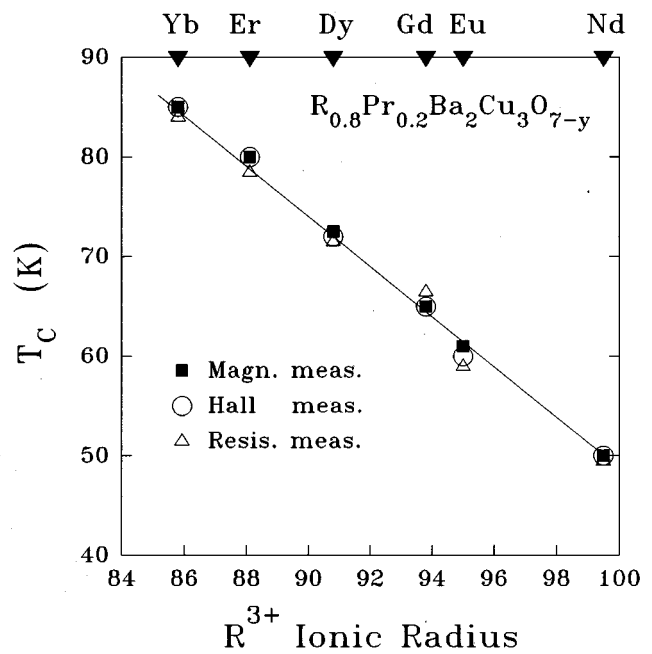


FIG. 4. T_c vs ionic radius of R^{3+} in $R_{0.8}\text{Pr}_{0.2}\text{Ba}_2\text{Cu}_3\text{O}_{7-y}$ ($R=\text{Yb, Er, Dy, Gd, Eu, Nd}$) systems.

in Fig. 5) the normal resistivity ρ_n increases linearly with increasing the R^{3+} ion size.

It is traditional to express a total electrical resistivity as the sum of two terms. One is the temperature-dependent term arising from the dynamic deviations from crystal perfection. Another is the temperature-independent residual resistivity arising from the static imperfections, such as impurities and lattice defects. The normal state resistivity ρ_n of $R_{0.8}\text{Pr}_{0.2}\text{Ba}_2\text{Cu}_3\text{O}_{7-y}$ in the temperature range 100–290 K could be fitted by the relation, $\rho_n(T)=\rho_0+aT$, where ρ_0 is the extrapolated value of ρ_n at $T=0$ and close to zero for undoped samples.

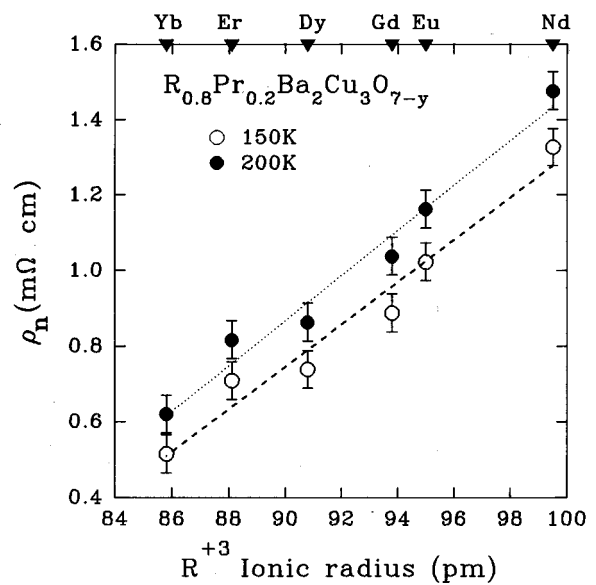


FIG. 5. ρ_n vs ionic radius of R^{3+} in $R_{0.8}\text{Pr}_{0.2}\text{Ba}_2\text{Cu}_3\text{O}_{7-y}$ ($R=\text{Yb, Er, Dy, Gd, Eu, Nd}$) systems.

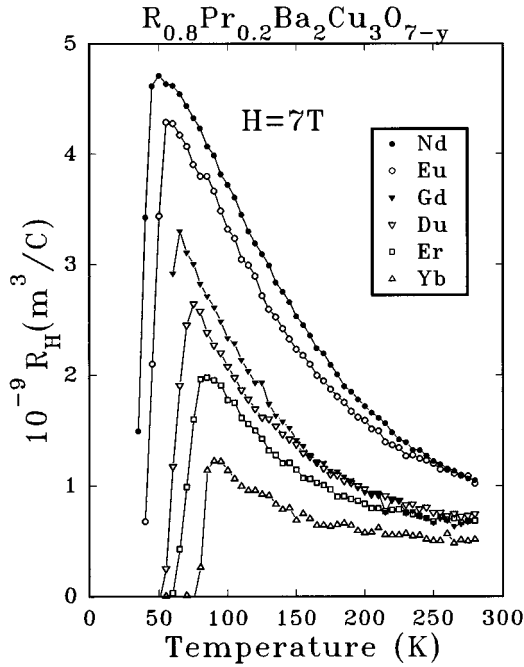


FIG. 6. Temperature dependence of the Hall coefficient, R_H , for $R_{0.8}\text{Pr}_{0.2}\text{Ba}_2\text{Cu}_3\text{O}_{7-y}$ ($R = \text{Yb, Er, Dy, Gd, Eu, Nd}$).

With increasing R^{3+} ion size, the resistivity curves $\rho_n(T)$ are shifted progressively upwards (Fig. 3), so that the primary effect of the R ion size is to add a nominally temperature-independent contribution, ρ_0 , to the transport scattering rate. This may be due to a progressive decrease in carrier concentration (our Hall measurements support this point of view), or/and a progressive increase of an unsuspected temperature-independent scattering (impurity scattering) contribution by increasing R^{3+} ion size in samples.

The slopes of the $\rho_n(T)$ curves, $d\rho_n/dT$, for different R -ion samples (Fig. 3) are nearly identical. This suggests that the ρ_0 is also R^{3+} ion size dependent. The ρ_0 is larger for compound with larger R^{3+} ion size. It is obvious that the R^{3+} ion size dependence of ρ_n is a consequence of the R^{3+} ion size dependence of ρ_0 .

Hall measurements were made with the same samples which we discussed above. Our results demonstrated that the Hall voltage V_{xy} at a constant temperature was linear in H and no saturation up to the maximum field of 7 Tesla.

The Hall coefficient R_H above T_c is holelike for all samples. The temperature dependence of R_H is shown in Fig. 6. The experimental values of R_H are in the range $0.5 \times 10^{-9} \text{ m}^3/\text{C}$ to $4.8 \times 10^{-9} \text{ m}^3/\text{C}$. R_H increases as the temperature decreases, and then drops sharply as the superconducting transition temperature is approached. Figure 4 also demonstrates that the T_c (onset) values obtained from the Hall measurements are in agreement with those from the magnetization and the resistivity measurements.

It is convenient to normalize the Hall constant to the unit cell volume V so that, in the case of a parabolic single band, the Hall number n_H (derived from $n_H = V/eR_H$) is the number of carriers per unit cell. The temperature dependence of the Hall number n_H is presented in Fig. 7.

As shown in Figs. 6 and 7, we find for $R_{0.8}\text{Pr}_{0.2}\text{Ba}_2\text{Cu}_3\text{O}_{7-y}$ systems, a nearly $1/T$ dependence of R_H and therefore, a nearly linear temperature dependence of

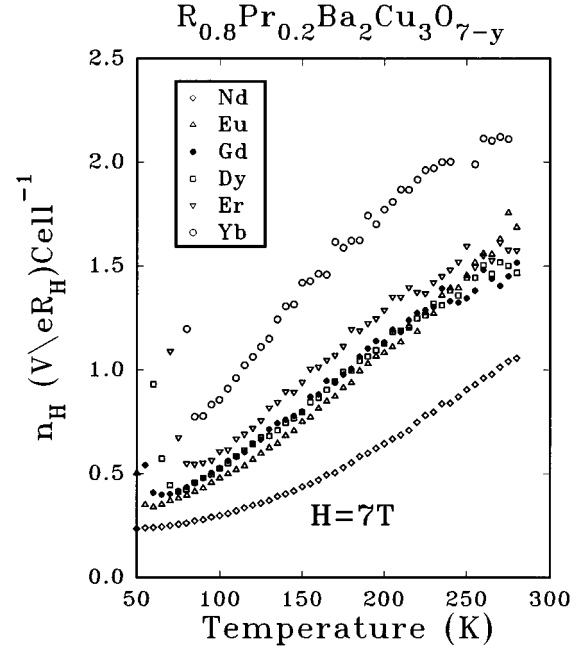


FIG. 7. Temperature dependence of the Hall number per unit cell volume V , n_H ($n_H = V/eR_H$), for $R_{0.8}\text{Pr}_{0.2}\text{Ba}_2\text{Cu}_3\text{O}_{7-y}$ ($R = \text{Yb, Er, Dy, Gd, Eu, Nd}$).

n_H , widely seen in many high- T_c cuprate superconductors.⁹⁻¹⁴

The transport measurements performed in sintered bulk samples are usually complicated by the character of the granularity in these samples (weak links between grains) and confused by anisotropic effect inside the grains. In spite of this, we believed that averaging data from several repeated measurements will merge reliable results.

For every $R_{0.8}\text{Pr}_{0.2}\text{Ba}_2\text{Cu}_3\text{O}_{7-y}$ compound, our Hall measurements were repeated on two samples with the same composition in order to double check for reproducibility. The typical results for $\text{Er}_{0.8}\text{Pr}_{0.2}\text{Ba}_2\text{Cu}_3\text{O}_{7-y}$ are shown in Fig. 8. The data points fall on a straight line in the temperature range approximately below 240 K. We have estimated the signal error of our system is about $10^{-7} \sim 10^{-8}$ V. However, the Hall voltage V_{xy} at low temperatures is in the order of 10^{-6} V and $V_{xy} \sim 1/T$. Therefore, above 240 K the Hall signals are small and sensitive to thermal shift during the measurements. We suspect this to be a serious source of error at higher temperature in these samples.

A very significant feature of the Hall effect data is the existence of a R^{3+} ion size effect on Hall number n_H in $R_{0.8}\text{Pr}_{0.2}\text{Ba}_2\text{Cu}_3\text{O}_{7-y}$ (Fig. 9). At a constant temperature the Hall number n_H decreases roughly linearly with increasing R^{3+} ionic radius.

It can be seen from Fig. 7 that for samples with smaller R^{3+} ionic radius (for example, $\text{Yb}_{0.8}\text{Pr}_{0.2}\text{Ba}_2\text{Cu}_3\text{O}_{7-y}$) n_H varies linearly with T down to a few degrees above T_c , but for samples with larger R^{3+} ionic radius (for example, $\text{Nd}_{0.8}\text{Pr}_{0.2}\text{Ba}_2\text{Cu}_3\text{O}_{7-y}$), the range of linearity shrinks.

A fundamental question for high- T_c cuprate superconductors is whether or not the normal state from which the superconducting one condenses is a Fermi liquid. One signature of the Fermi liquid state is a quadratic dependence of electrical resistivity on temperature below the range in which

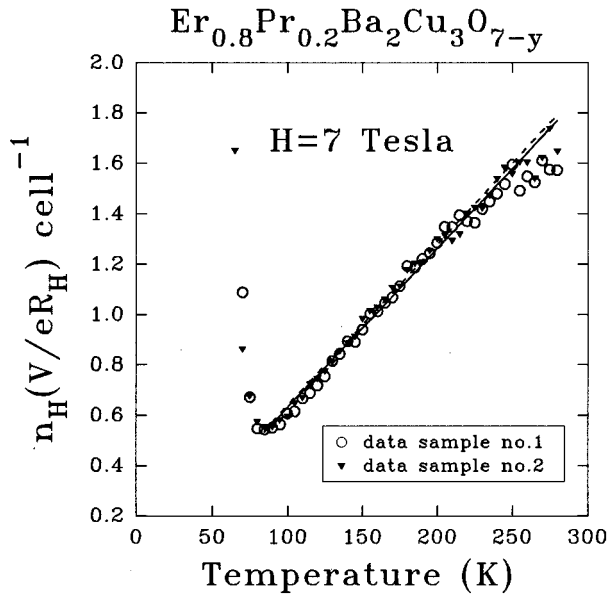


FIG. 8. Temperature dependence of the Hall number per unit cell volume V , $n_H (n_H \equiv V/eR_H)$, for $\text{Er}_{0.8}\text{Pr}_{0.2}\text{Ba}_2\text{Cu}_3\text{O}_{7-y}$ (sample no. 1 and sample no. 2 were prepared under the same conditions).

phonon scattering dominates. The linear temperature dependence of the resistivity and Hall number appears implying a breakdown of the Fermi-liquid description.

Anderson has proposed a theory in the framework of the two-dimensional Luttinger liquid.⁸ In his picture two types of quasiparticle excitations, spinons and holons, and two different relaxation times, τ_{tr} and τ_H , have been introduced. The relaxation rates for carrier motion normal to the Fermi surface ($1/\tau_{tr}$) is the usual transport relaxation rate. It is related to the spinon-holon scattering which leads to a linear T de-

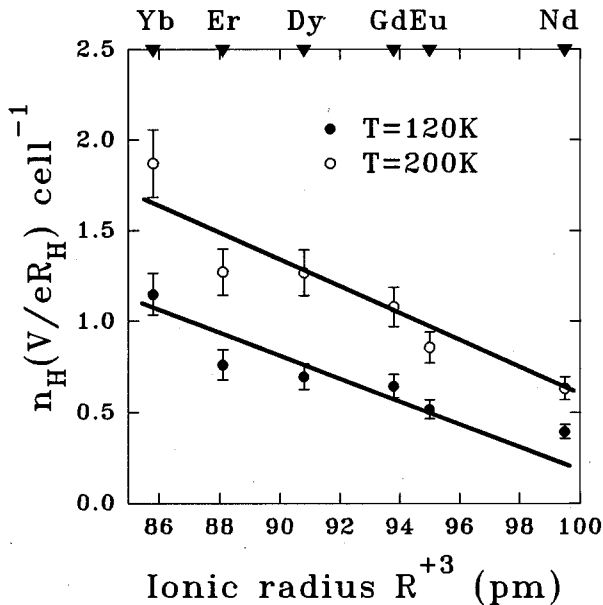


FIG. 9. The Hall number per unit cell volume V , $n_H (n_H \equiv V/eR_H)$, vs ionic radius of R^{3+} in $\text{R}_{0.8}\text{Pr}_{0.2}\text{Ba}_2\text{Cu}_3\text{O}_{7-y}$ ($R = \text{Yb}, \text{Er}, \text{Dy}, \text{Gd}, \text{Eu}, \text{Nd}$) systems.

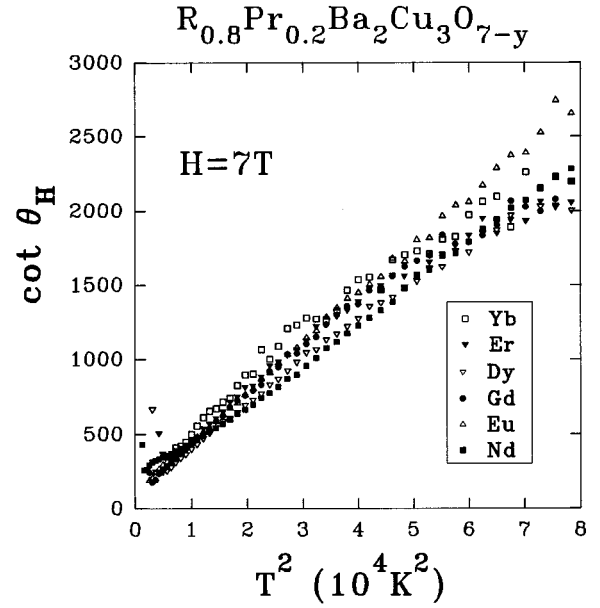


FIG. 10. The variation of cotangent Hall angle $\cot\theta_H$ with T^2 for $\text{R}_{0.8}\text{Pr}_{0.2}\text{Ba}_2\text{Cu}_3\text{O}_{7-y}$ ($R = \text{Yb}, \text{Er}, \text{Dy}, \text{Gd}, \text{Eu}, \text{Nd}$).

pendence, i.e., $\tau_{tr} \propto 1/T$, and determines the longitudinal conductivity $\sigma_{xx} \propto \tau_{tr} \propto 1/T$. The relaxation time for carrier motion parallel to the Fermi surface, τ_H , is the transverse (Hall) relaxation time. It is the result of the scattering between spinons alone which varies as $\tau_H \propto 1/T^2$. Thus, $\sigma_{xy} \sim \tau_H \tau_{tr} \sim 1/T^3$. The cotangent of the Hall angle becomes one of the essential quantities since it is dependent on τ_H only:

$$\cot(\theta_H) = \sigma_{xx}/\sigma_{xy} = 1/\omega_c \tau_H = \alpha T^2 + C, \quad (1)$$

where α is related to the spinon bandwidth W_s ($\alpha \propto W_s^{-1}$), and C is an additive term due to magnetic impurity scattering.

The simultaneous measurements of the Hall resistivity $\rho_{xy} \equiv R_H H$ and magnetic resistivity ρ_{xx} in field of 7 Tesla enable us to calculate accurately the cotangent of the Hall angle, $\cot\theta_H (= \rho_{xx}/\rho_{xy})$. A universal quadratic temperature dependence of $\cot\theta_H$ is preserved in all samples of $\text{R}_{0.8}\text{Pr}_{0.2}\text{Ba}_2\text{Cu}_3\text{O}_{7-y}$ systems (Fig. 10). The fan-shaped $\cot\theta_H(T^2)$ curves in Fig. 10 is a result from the fluctuation of signals at higher temperatures. The intercepts C and the slopes α remain almost constant within small fluctuations. The slope α as a function of the R^{3+} ionic radius is shown in Fig. 11.

Both ρ_{xx} and ρ_{xy} are approximately linearly with R^{3+} ionic radius (see Figs. 6 and 7), however, it seems that these two effects combine to weaken the ionic size dependence of $\cot\theta_H (= \rho_{xx}/\rho_{xy})$.

Earlier Hall measurements⁹⁻¹⁴ on 123-type high- T_c superconductors reveal that Eq. (1) seems to be universal in every system with different dopant and doping levels. However, the behavior of the slope α and intercept C are quite different for different systems.

For the case of in-plane zinc dopants in crystals of $\text{YBa}_2(\text{Cu}_{1-x}\text{Zn}_x)_3\text{O}_{7-\delta}$ (Ref. 12), C in Eq. (1) linearly increases with increasing zinc concentration, but the parameter α is essentially unchanged, consistent with the interpretation that Zn is an in-plane scatterer and pair breaker¹² which has

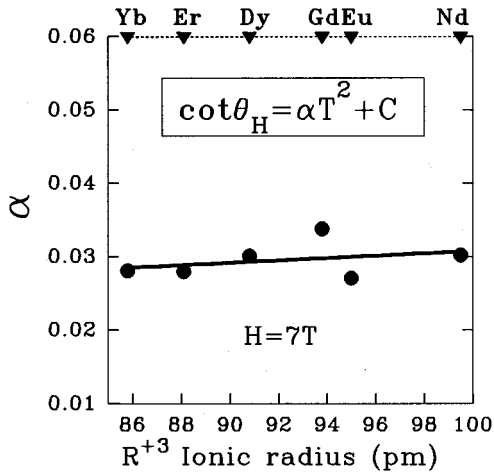


FIG. 11. The slope α of the curve $\cot \theta_H(T^2)$ vs ionic radius of R^{3+} in $R_{0.8}\text{Pr}_{0.2}\text{Ba}_2\text{Cu}_3\text{O}_{7-y}$ ($R=\text{Yb, Er, Dy, Gd, Eu, Nd}$) systems.

little effect on the carrier concentration. For the case of CuO-chain-sites cobalt doping in crystals of $\text{YBa}_2(\text{Cu}_{1-x}\text{Co}_x)_3\text{O}_{7-\delta}$ (Ref. 13), Co doping is thought to change the T_c by changing the hole concentration.¹⁵ The results showed that doping with Co decreases α while leaving the residual scattering parameter C unchanged.

For the case of oxygen-deficient $\text{YBa}_2\text{Cu}_3\text{O}_{7-\delta}$ epitaxial films,⁹ the oxygen reduction (an increase in δ), as in the case of Co doping, is thought to change the T_c by changing the hole concentration. However, the results showed that oxygen reduction increases α , leaving the residual scattering parameter C unchanged.

For the case of the Y-site doping by Pr in $\text{Y}_{1-x}\text{Pr}_x\text{Ba}_2\text{Cu}_3\text{O}_{7-\delta}$ epitaxial films,⁹ both α and C increase with Pr concentration x . These results support the view that hybridization exists between Pr 4f states and the CuO_2 plane electronic states, causing the Pr magnetic moment to become effective scatterer to the electron transport. The scattering by these moments reduces the carrier mobility, which corresponds to an increase in C . On the other hand, the increase in the slope α indicates a drop in the true carrier density. These results imply that a combination of magnetic impurity scattering and hole filling (hole localization) is the mechanism for the suppression of superconductivity in $\text{Y}_{1-x}\text{Pr}_x\text{Ba}_2\text{Cu}_3\text{O}_{7-y}$.

All of the Hall experiments above⁹⁻¹⁴ reveal a unified picture of Hall effect in various high- T_c cuprate systems. While the increase of C corresponds to a reduction of mobility, the change of α reflects the variation in true carrier density.⁹

All of the Hall experiments above⁹⁻¹⁴ have focused on the change of the concentration x of the dopants or the oxygen reduction δ , we carried out present Hall measurements in $R_{0.8}\text{Pr}_{0.2}\text{Ba}_2\text{Cu}_3\text{O}_{7-y}$ systems, in which instead of changing the concentration, we change the R^{3+} ion while leaving the concentration of Pr and oxygen unchanged.

Our results are obviously different from those obtained from all the other systems. In our case both parameters α and C , in formula of $\cot(\theta_H) = \rho_{xx}/\rho_{xy} = \alpha T^2 + C$, remain almost constant and do not change with the changing of R in $R_{0.8}\text{Pr}_{0.2}\text{Ba}_2\text{Cu}_3\text{O}_{7-y}$, although both magnetic and Hall resistivity, ρ_{xx} and ρ_{xy} , are significantly R^{3+} ion size dependent.

A significant controversy arises over the role of parameters α and C in Eq. (1) by comparing our results in $R_{0.8}\text{Pr}_{0.2}\text{Ba}_2\text{Cu}_3\text{O}_{7-y}$ with results obtained in other systems.⁹⁻¹⁴

In a unified picture of Hall effect as mentioned above, parameter C is a measure of the in-plane impurity scattering rate. It is not surprising that C is independent of R^{3+} ion substituted in Y site in $R_{0.8}\text{Pr}_{0.2}\text{Ba}_2\text{Cu}_3\text{O}_{7-y}$. (The Pr ion also was substituted in the Y site, due to its hybridization with CuO_2 planes it could reduce carrier mobility by the magnetic scattering, causing an increase in parameter C .) On the other hand, ρ_0 is also a measure of the in-plane impurity scattering rate, but as shown in Fig. 5 it is strongly R^{3+} ion size dependent.

The change of α was attributed to the variation in the true carrier density.⁹ However, we observed that although the Hall number n_H decreases with increasing R^{3+} ion size while the parameter α does not change with R^{3+} ion in $R_{0.8}\text{Pr}_{0.2}\text{Ba}_2\text{Cu}_3\text{O}_{7-y}$ systems.

As mentioned earlier, we observed a strong R^{3+} ion-size effect on T_c (Fig. 4), ρ_n (Fig. 5) and n_H (Fig. 9) in $R_{0.8}\text{Pr}_{0.2}\text{Ba}_2\text{Cu}_3\text{O}_{7-y}$. However, the Hall angle remains almost constant when we change the rare-earth ion in sample of $R_{0.8}\text{Pr}_{0.2}\text{Ba}_2\text{Cu}_3\text{O}_{7-y}$. On the contrary to the conclusion in a number of previous studies,⁹⁻¹⁴ our results strongly suggest that there is no simple correlation between the Hall angle in the normal state, including the parameters α and C , with superconductivity (T_c) in 123-type high- T_c superconductors.

It should also be noted that a band model involving a square Fermi surface with rounded corners could also lead to the above T^2 law.^{16,17} Therefore, one cannot conclude the validity of Anderson's picture simply based on the applicability of Eq. (1) to the observed results.

It has been well established that holes are the superconducting elements in the P -type high- T_c cuprate superconductors, and are mainly confined to the two-dimensional CuO_2 sheet.¹⁸ The high- T_c cuprate superconductors have been known to have a strong dependence of T_c on the hole content and a certain similar trend between T_c and the hole content exists in these individual series compounds.¹⁹ High transition temperatures are found in a somewhat narrow window of hole concentration.

Several authors¹⁹ suggested that T_c is an inverted parabolic function of carrier concentration in both the underdoped and the overdoped regions, i.e.,

$$T_c = T_{c,\text{max}}[1 - \eta(n - n_{\text{opt}})^2], \quad (2)$$

where $T_{c,\text{max}}$ is the maximum T_c at the optimal doping level n_{opt} . Such an empirical relation was well established in the case of Sr substituted La_2CuO_4 .

Recently, Zhang and Sato²⁰ suggested a universal relationship between the normalized T_c and the hole content p_{sh} (p_{sh} is defined as the number of holes per CuO_2 unit in the 2D layer). The universal curve is characterized by a plateau ($0.12 < p_{\text{sh}} < 0.25$) with sharp bends at underdoped side ($0.06 < p_{\text{sh}} < 0.12$) and overdoped side ($0.25 < p_{\text{sh}} < 0.31$).

In both pictures mentioned above the hole concentration p_{sh} in the covalent CuO_2 sheets is given by conservation of charge. For a giving compound p_{sh} is a constant and essentially independent on the temperature. p_{sh} was measured by chemical methods (titration technique) or calculated by

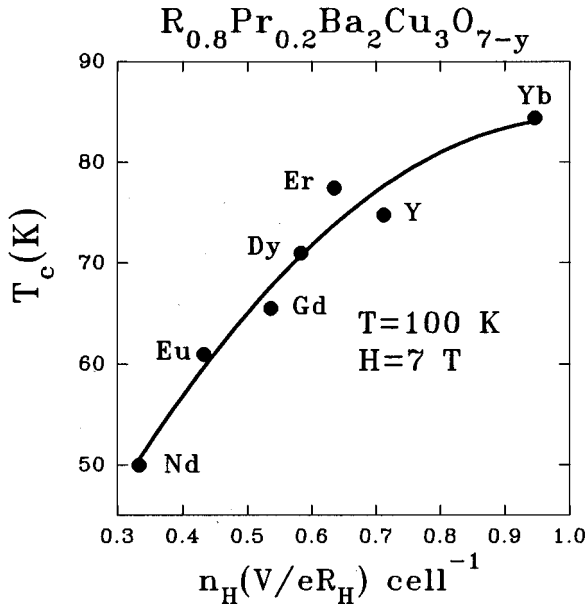


FIG. 12. The T_c - n_H (n_H at $T=100$ K) diagram illustrating an underdopinglike behavior in $R_{0.8}\text{Pr}_{0.2}\text{Ba}_2\text{Cu}_3\text{O}_{7-y}$ ($R=\text{Yb, Er, Dy, Gd, Eu, Nd}$) systems.

Rietveld analyses using a bond valence sum (BVS) model.²¹ The chemical analyses should give a total number of charge in compounds and the BVS for the copper atoms should be taken to represent also the total charge in the bond.

p_{sh} reflects the total number of the hole density which are not matched with Hall number n_H . n_H is related only to the “moving holes.” In an isotropic parabolic single-band Fermi liquid system, the Hall number, $n_H = V/eR_H$ would be the number of carriers per unit cell. For the high- T_c cuprate superconductors, due to its T dependence and the complex band structure, n_H may not represent the actual carrier concentration. However, the value of n_H at a particular T correlates rather consistently with the carrier concentration determined by other methods, n_H scales with actual carrier concentration.

On the basis of our Hall effect measurements, we also found an empirical relation between the superconducting transition temperature T_c and the mobile carrier concentration n_H . Figure 12 presents the T_c as a function of the Hall number n_H (n_H at $T=100$ K) for $R_{0.8}\text{Pr}_{0.2}\text{Ba}_2\text{Cu}_3\text{O}_{7-y}$ systems. The T_c - n_H diagram (Fig. 12) manifests an “underdoping” behavior. The values of n_H at 100 K for several compounds fall out the limits of the superconducting window ($0.06 < p_{\text{sh}} = 1/2 n_H < 0.31$). The word “underdoping” is usually used in the case of the doping content below the optimum concentration, but in our case we only change the R ion in sample of $R_{0.8}\text{Pr}_{0.2}\text{Ba}_2\text{Cu}_3\text{O}_{7-y}$ while the composition remains constant. Our data established that the substitution by a R ion with larger ionic radius in $R_{0.8}\text{Pr}_{0.2}\text{Ba}_2\text{Cu}_3\text{O}_{7-y}$ is equivalent to increasing the Pr concentration in it.

In literature the Hall effect measurements on $\text{Y}_{1-x}\text{Pr}_x\text{Ba}_2\text{Cu}_3\text{O}_{7-\delta}$ have been interpreted in the light of the “valent” model,^{1,22} because a decrease of the Hall number n_H with the increase of Pr content has been observed. The strong T dependence of n_H in Fig. 9 complicates a determination of the true carrier density from n_H . Therefore, the decrease of n_H with x does not provide conclusive evidence

for hole filling by the Pr dopant. The phenomena are connected not to the Pr^{4+} content, but to the “moving holes.” It should be emphasized that the Hall number n_H changes by a factor of 2 from $\text{Yb}_{0.8}\text{Pr}_{0.2}\text{Ba}_2\text{Cu}_3\text{O}_{7-y}$ to $\text{Nd}_{0.8}\text{Pr}_{0.2}\text{Ba}_2\text{Cu}_3\text{O}_{7-y}$ in all temperature region 100–280 K (Fig. 7). Within the framework of the “valent” model one expects the $n_H(T)$ dependence for the Yb and the Nd-based systems to be close to each other.

The suppression of T_c in $R_{1-x}\text{Pr}_x\text{Ba}_2\text{Cu}_3\text{O}_{7-y}$ has been attributed to two possible mechanisms: the pair-breaking²³ and/or hole localization,⁶ both due to hybridization of the Pr ion with the sandwiching CuO_2 planes. Fehrenbacher and Rice²⁴ proposed a model for the electronic structure of $\text{PrBa}_2\text{Cu}_3\text{O}_7$. The difference between $\text{PrBa}_2\text{Cu}_3\text{O}_7$ and other $R\text{Ba}_2\text{Cu}_3\text{O}_7$ superconductors comes from an enhanced stability of the Pr^{IV} state due to the hybridization with oxygen neighbors, and involves a transfer of holes from primarily planar $\text{O } 2p\sigma$ to $\text{O } 2p\pi$ states. The resulting hybridized state is a mixture of Pr^{4+} and Pr^{3+} + ligand hole, i.e., the wave function has the form

$$|\Psi\rangle = \alpha|4f^1p^6\rangle + \beta|4f^2p^5\rangle. \quad (3)$$

If the weight of the β of the $(\text{Pr}^{3+} \text{L})$ state is large, many local properties of Pr, as seen by high-energy spectroscopy, would be similar to those of Pr^{3+} . Furthermore, the orbital of $4f$ wave functions of the Pr ions are more spatially extended (Pr^{3+} is the largest paramagnetic rare earth that forms in the Y-Ba-Cu-O structure). This fact could enhance the hybridization between Pr orbital states and the valence band states associated with the CuO_2 planes. Hybridization could generate an exchange interaction between the Pr magnetic moments and the spin of the mobile holes in the CuO_2 planes.²⁴ This superexchange interaction between conducting holes and Pr magnetic moment in $R_{1-x}\text{Pr}_x\text{Ba}_2\text{Cu}_3\text{O}_{7-y}$ systems is probably the mechanism of the pair-breaking and the hole localization (the reduction of the number of mobile holes n_H) leading to the T_c suppression.

The $4f$ wave function of the R (except Pr) ions with a symmetry different from Pr and with a smaller spatial extension does not lead to appreciable hybridization with the valence band states associated with the CuO_2 planes. The conduction holes in the CuO_2 planes have almost zero density of states at the R ion sites.²⁵ The R ions and the CuO_2 layers are electronically decoupled.²⁶ The moment of R ions in $R_{1-x}\text{Pr}_x\text{Ba}_2\text{Cu}_3\text{O}_{7-y}$ could not give an effect of pair-breaking or hole localization. However, the spatial extent of R ions (ionic radius) could produce a strong effect on the hybridization between valence band states of CuO_2 planes and Pr $4f$ states. For R ions with a larger ionic radius in $R_{1-x}\text{Pr}_x\text{Ba}_2\text{Cu}_3\text{O}_{7-y}$, we observed a stronger T_c suppression by doping with the same Pr concentration. This is due to that the R ion with a larger ionic radius could enhance more strongly the hybridization between Pr orbital states and the valence band states of CuO_2 planes.

We propose that as doping Pr in $R\text{Ba}_2\text{Cu}_3\text{O}_{7-y}$ the hybridization between Pr $4f$ states and valence band states in the CuO_2 planes provide an additional local impurity magnetic scattering by moment of Pr ions for resistivity (Kondo-like mechanism), and that the hybridization would result in localization of the mobile holes (the reduction of the number

of mobile holes n_H) in the CuO_2 planes. On the basis of our experiments both effects could be R ion-size dependent.

There is one difficulty to reconcile the trend in the behavior of Pr in different hosts $R\text{Ba}_2\text{Cu}_3\text{O}_{7-y}$ with the hybridization picture. For example, the T_c values and the critical concentration of Pr, x_{cr} , necessary to suppression superconductivity are found to decrease with the increase of R^{3+} radius. One would expect the opposite effect based on the hybridization picture since increasing radius of rare earth R^{3+} , the average distance between CuO_2 planes becomes larger which leads to a weaker Pr-CuO₂ hybridization.

It is established²⁷ that the distance between Pr and the surrounding oxygen $d_{\text{Pr-O}}$ is less than $d_{\text{Y-O}}$ (most probably due to p - f hybridization). It is also known that increased local buckling of CuO_2 planes suppresses T_c and inhibits metallic conductivity. Thus if the $d_{\text{Pr-O}}$ is the same in all hosts one would have stronger buckling around Pr for larger host R ions.

On the basis of our x-ray diffraction data, especially noteworthy is that the increase of c axis from 11.654 Å for $\text{Yb}_{0.8}\text{Pr}_{0.2}\text{Ba}_2\text{Cu}_3\text{O}_{7-y}$ to 11.748 Å for $\text{Nd}_{0.8}\text{Pr}_{0.2}\text{Ba}_2\text{Cu}_3\text{O}_{7-y}$ is less than that of the ionic radii from 0.858 Å for Yb^{3+} to 0.995 Å for Nd^{3+} . The lattice undergoes a monotonic compression when the Y site in 123 series is substituted by R^{3+} with larger radius. All these facts may be connected with the increase of Pr-CuO₂ hybridization and the role of localization with enlargement of R^{3+} ion radius.

Recently Norton *et al.* reported the results of the investigation of the transport and structural properties of $\text{Pr}_{1-x}\text{Ca}_x\text{Ba}_2\text{Cu}_3\text{O}_{7-y}$ thin films.²⁸ Their results support the view that hole localization, due to hybridization of the Pr $4f$ electronic levels with the O $2p$ orbitals, contributes substan-

tially to the suppression of superconductivity by Pr in $\text{PrBa}_2\text{Cu}_3\text{O}_{7-y}$, and demonstrates that this suppression can be partially compensated by appropriate hole doping with Ca.

In conclusion, we find a linear temperature dependence of the normal state resistivity ρ_n and the Hall number n_H in bulk $R_{0.8}\text{Pr}_{0.2}\text{Ba}_2\text{Cu}_3\text{O}_{7-y}$ samples ($R = \text{Yb, Er, Dy, Gd, Eu, and Nd}$). At a constant temperature both ρ_n and n_H are linearly dependent on ion size of rare earth. The cotangent of the Hall angle follows a universal T_2 dependence. Both the slope α and the quantity C is insensitive to R ions and remains almost constant. We proposed a T_c - n_H diagram which manifests an “underdoping” behavior of $R_{0.8}\text{Pr}_{0.2}\text{Ba}_2\text{Cu}_3\text{O}_{7-y}$ systems. We suggest that the strong hybridization between $4f$ states of the Pr ion and the conduction band states in CuO_2 planes, leading to the hole localization and the pair breaking, are the mechanism for the suppression of superconductivity and the mechanism for the increase of resistivity ρ_n and reduction of the number of mobile holes n_H in the normal state in $R_{1-x}\text{Pr}_x\text{Ba}_2\text{Cu}_3\text{O}_{7-y}$ systems. Especially noteworthy is that the R ion with a larger radius could more strongly enhance the hybridization between Pr orbital states and the valence band states of CuO_2 planes. This is a natural explanation of the rare-earth ion size effect on T_c, T_N, ρ_n , and n_H , which we observed in the last several years.

ACKNOWLEDGMENTS

We thank S. H. Cheng and L. C. Tung for helpful discussions. This study was supported by the National Science Council, R. O. C. Grant No. NSC90208M00795.

- ¹H. B. Radousky, *J. Mater. Res.* **7**, 1917 (1992).
- ²A. Kebede, C.-S. Jee, J. Schwegler, J. E. Crow, T. Mihalisin, G. H. Myer, R. E. Solomon, P. Schlottmann, M. V. Kuric, S. H. Bloom, and R. P. Guertin, *Phys. Rev. B* **40**, 4453 (1989).
- ³W. H. Li, J. W. Lynn, S. Skanthakumar, T. W. Clinton, A. Kebede, C.-S. Jee, J. E. Crow, and T. Mihalisin, *Phys. Rev. B* **40**, 5300 (1989).
- ⁴Yunhui Xu and Weiyang Guan, *Solid State Commum.* **80**, 105 (1991); Yunhui Xu and Weiyang Guan, *Phys. Rev. B* **45**, 3176 (1992).
- ⁵Weiyang Guan, Y. C. Chen, J. Y. T. Wei, Yunhui Xu, and M. K. Wu, *Physica C* **209**, 19 (1993); Weiyang Guan and Yunhui Xu, S. R. Sheen, Y. C. Chen, J. Y. T. Wei, H. F. Lai, and M. K. Wu, *Phys. Rev. B* **49**, 15 993 (1994).
- ⁶Weiyang Guan, *Chin. J. Phys.* **31**, 849 (1993); Weiyang Guan, *Physica C* **235-240**, 781 (1994).
- ⁷P. P. Allen, Z. Fisk, and A. Migliori, in *Physical Properties of High Temperature Superconductors I*, edited by D. M. Ginsberg (World Scientific, Singapore, 1989), Vol. 1, p. 213.
- ⁸P. W. Anderson, *Phys. Rev. Lett.* **67**, 2092 (1991).
- ⁹Peng Xiong and Gang Xiao, *Phys. Rev. B* **47**, 5516 (1993).
- ¹⁰J. R. Cooper, S. D. Obertelli, A. Carrington, and J. W. Loram, *Phys. Rev. B* **44**, 12 086 (1991); J. M. Harris, Y. F. Yan, and N. P. Ong, *ibid.* **46**, 14 293 (1992); B. Wuyts, E. Osquiguil, M. Maenhoudt, S. Libbrecht, Z. X. Gao, and Y. Bruynseraede, *ibid.* **47**, 5512 (1993); E. C. Jones, D. K. Christen, J. R. Thompson, R. Freenstra, S. Zhu, D. H. Lowndes, J. M. Phillips, M. P. Siegal, and J. D. Budai, *ibid.* **47**, 8986 (1993); R. Hopfengartner, M. Lippert, W. Dorsch, H. Dirtrich, G. Kreiselmeyer, and G. Saaemann-Ischenko, *J. Supercond.* **7**, 319 (1994); M. S. Raven and Y. M. Wan, *Phys. Rev. B* **51**, 561 (1995).
- ¹¹A. Matsuda, K. Kinoshita, T. Ishii, H. Shibata, T. Watanabe, and T. Yamada, *Phys. Rev. B* **38**, 2910 (1988); Wu Jiang, J. L. Peng, S. J. Hagen, and R. L. Green, *ibid.* **46**, 8694 (1992); V. N. Narozhnyi, *Supercond. Phys. Chem. Technol.* **7**, 571 (1994).
- ¹²T. R. Chien, Z. Z. Wang, and N. P. Ong, *Phys. Rev. Lett.* **67**, 2088 (1991); G. Ilonca, M. Mehbod, A. Lanckbeem, and R. Deltour, *Phys. Rev. B* **47**, 15 265 (1993).
- ¹³A. Carrington, A. P. Mackenzie, C. T. Lin, and J. R. Cooper, *Phys. Rev. Lett.* **69**, 2855 (1992).
- ¹⁴G. Kallias, I. Panagiotopoulos, D. Niarchos, and A. Kostikas, *Phys. Rev. B* **48**, 15 992 (1993).
- ¹⁵J. Clayhold, S. Hagen, Z. Z. Wang, N. P. Ong, J. M. Tarascon, and P. Barboux, *Phys. Rev. B* **39**, 777 (1989).
- ¹⁶A. S. Alexandrov, A. M. Bratkovsky, and N. F. Mott, *Phys. Rev. Lett.* **72**, 1734 (1994).
- ¹⁷W. E. Pickett, H. Krakauer, R. E. Cohen, and D. J. Singh, *Science* **255**, 46 (1992).
- ¹⁸S. Martin, A. T. Fiory, R. M. Fleming, L. F. Schneemeyer, and J. V. Waszczak, *Phys. Rev. Lett.* **60**, 2194 (1988).

- ¹⁹J. B. Torrance, Y. Tokura, A. I. Nazzal, A. Bezinge, T. C. Huang, and S. S. P. Parkin, *Phys. Rev. Lett.* **61**, 1127 (1988); J. B. Torrance *et al.*, *Physica C* **162-164**, 291 (1989); M. H. Whangbo and C. C. Torardi, *Science* **249**, 1143 (1990); C. N. R. Rao *et al.*, *Physica C* **174**, 11 (1991).
- ²⁰H. Zhang and Hiroshi Sato, *Phys. Rev. Lett.* **70**, 1697 (1993).
- ²¹I. D. Brown, *J. Solid State Chem.* **82**, 122 (1989); I. D. Brown, *J. Solid State Chem.* **90**, 155 (1991).
- ²²J. J. Neumeier, T. Björnholm, M. B. Maple, and Ivan K. Schuller, *Phys. Rev. Lett.* **63**, 2516 (1989).
- ²³Yunhui Xu and Weiyuan Guan, *Appl. Phys. Lett.* **59**, 2183 (1991); Yunhui Xu and Weiyuan Guan, *Phys. Lett. A* **163**, 104 (1992); Yunhui Xu and Weiyuan Guan, *Physica C* **183**, 105 (1991).
- ²⁴R. Fehrenbacher and T. M. Rice, *Phys. Rev. Lett.* **70**, 3471 (1993).
- ²⁵J. Yu, S. Massidda, and A. J. Freeman, *Phys. Lett. A* **122**, 203 (1987).
- ²⁶Yunhui Xu and Weiyuan Guan, *Appl. Phys. Lett.* **53**, 334 (1988).
- ²⁷M. E. Lopez-Morales *et al.*, *Phys. Rev. B* **41**, 6655 (1990).
- ²⁸D. P. Norton, D. H. Lowndes, B. C. Sales, J. D. Budai, E. C. Jones, and B. C. Chakoumakos, *Phys. Rev. B* **49**, 4182 (1994).